



GLOBAL JOURNAL OF RESEARCHES IN ENGINEERING: B
AUTOMOTIVE ENGINEERING
Volume 16 Issue 1 Version 1.0 Year 2016
Type: Double Blind Peer Reviewed International Research Journal
Publisher: Global Journals Inc. (USA)
Online ISSN: 2249-4596 & Print ISSN: 0975-5861

Investigations on the Potential of Miller Cycle for Performance Improvement of Gas Engine

By Haijun Mo, Yongquan Huang, Xiaojian Mao & Bin Zhuo
Shanghai Jiao Tong University

Abstract- To further improve thermal efficiency, Miller Cycle was applied to a turbo-charged 338 kW gas engine. Different methods of Miller Cycle were analyzed, including three Early Intake-Valve Closing (EIVC) methods and three Late Intake-Valve Closing (LIVC) methods. After the relatively suitable methods were chosen, the combination of the Miller Cycle and higher compression ratio was extensively investigated. The experimental results demonstrated that the combination of intake valves closing 40°CA earlier (EIVC40) and the compression ratio increasing to 13, the maximum thermal efficiency reached 47% and it is about 5~7% higher than the original cycle.

Keywords: miller cycle, compression ratio, thermal efficiency, performance.

GJRE-B Classification: FOR Code: 090203



Strictly as per the compliance and regulations of :



© 2016. Haijun Mo, Yongquan Huang, Xiaojian Mao & Bin Zhuo. This is a research/review paper, distributed under the terms of the Creative Commons Attribution-Noncommercial 3.0 Unported License <http://creativecommons.org/licenses/by-nc/3.0/>, permitting all non commercial use, distribution, and reproduction in any medium, provided the original work is properly cited.

Investigations on the Potential of Miller Cycle for Performance Improvement of Gas Engine

Haijun Mo ^α, Yongquan Huang ^ο, Xiaojian Mao ^ρ & Bin Zhuo ^ω

Abstract- To further improve thermal efficiency, Miller Cycle was applied to a turbo-charged 338 kW gas engine. Different methods of Miller Cycle were analyzed, including three Early Intake-Valve Closing (EIVC) methods and three Late Intake-Valve Closing (LIVC) methods. After the relatively suitable methods were chosen, the combination of the Miller Cycle and higher compression ratio was extensively investigated. The experimental results demonstrated that the combination of intake valves closing 40°CA earlier(EIVC40) and the compression ratio increasing to 13, the maximum thermal efficiency reached 47% and it is about 5~7% higher than the original cycle.

keywords: miller cycle, compression ratio, thermal efficiency, performance.

NOMENCLATURE

CA : crank angle
EIVC : early intake-valve closing
LIVC : late intake-valve closing
BDC : bottom dead center
ABDC : after bottom dead center

I. INTRODUCTION

Natural gas is a relatively clean alternative energy, but the higher ignition temperature, the slower flame propagation speed and the smaller coefficient of molecular after the combustion all result in lower thermal efficiency. One effective way to improve the thermal efficiency of the engine is to increase the compression ratio. But for natural gas engines, the combustion temperature will increase when the compression ratio is higher, which leads to the increase of knocking tendency, reducing the reliability and service life of the engine. To avoid knocking, the general measure is to delay the ignition timing that will cancel out the improving of thermal efficiency caused by the increase of the compression ratio [1, 2].

Changing the intake valve closing time so the mixture in cylinder goes through an expansion process before the compression stroke, Miller cycle can decrease the maximum combustion temperature to some extent, combined with a higher compression ratio; it can improve the thermal efficiency. In this paper, the

engine performance of applying the Miller cycle on a nature gas engine was studied by simulation, and optimized by different levels of compression ratio. Simulation results indicated that the combination of intake valves closing 40°CA earlier(EIVC40) and the compression ratio increasing to 13 was the most potential method to further improve thermal efficiency, and experimental results proved that the method made engine fuel consumption rate got worse at high engine speeds but improved at media and low speeds, the engine knocking tendency increased at the same time.

II. CONCEPT OF MILLER CYCLE

In comparison with the standard cycles, miller cycle is shown in Figure 1 (a). Standard cycle of a gas engines is 1-5-2-3-4-6-7-1, 1-5 is the intake stroke, after the piston moves down to the bottom dead center (point 5) the intake valves are closed; 5-2 is the compression stroke; 2-3-4 is the expansion stroke; 4-6-7 is the exhaust stroke.

EIVC Miller cycle is 1-1a-5a-2a-3a-4a-6-7-1, 1-1a is the intake stroke, the intake valves are closed at point 1a, the piston continues to move down to the bottom dead center(BDC) which is denoted by point 5a, from 1a to 5a the in-cylinder mixture expands, which makes the in-cylinder temperature drops, so when the piston reach BDC, the temperature of the charge is lower in the Miller cycle compared to the standard cycle; the compression stroke is 5a-2a, the temperature of the charge at the point of 2a is also lower, so does the pressure; the expansion stroke is 2a-3a-4a, burst pressure and maximum combustion temperature are relatively low in miller cycle; the exhaust stroke is 4a-6-7.

Another form of Miller cycle is late intake-valve closing (LIVC), as Figure 1 (b) shows, the intake valves which should be closed at point 5 are postponed to point 1, LIVC makes the expansion ratio greater than the compression ratio, and extract heat from fuel as much as possible, which will improve the thermal efficiency.

Author α: School of Mechanical Engineering, Shanghai Jiao Tong University, Shanghai, China, College of Mechanical Engineering, GuanXi University, Nanning, China. e-mail: cherrymhj@163.com

Author ο: Yuchai Machinery Co.,Ltd, No.88 Tianqiao West Road, Yulin, Guangxi, China

Author ρ ω: School of Mechanical Engineering, Shanghai Jiao Tong University, Shanghai, China.

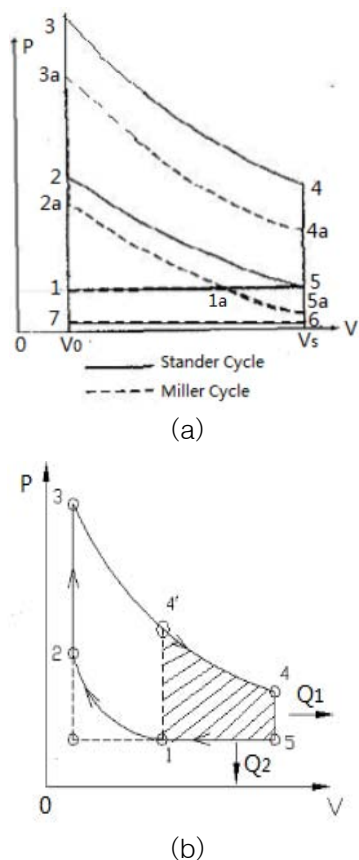


Figure 1: Theoretical Indicator Card of Miller Cycle

III. CALCULATION OF MILLER CYCLE

From the thermodynamic point of view, Miller cycle reduces the combustion temperature, which helps to decrease knock tendency and make it possible to raise the compression ratio. In addition, Miller cycle changes the intake quantity which also has impact on the combustion process. In order to optimize the performance, one-dimensional and multi-dimensional numerical modes are set up to study the in-cylinder gas flow and heat release in a gas engine, together with experimental results. The parameters of the gas engine are shown in Table 1.

Table 1: The Main Technical Parameters of the Engine

| | |
|---------------------|--------|
| Number of Cylinders | 6 |
| Bore/ mm | 129 |
| stroke/ mm | 165 |
| displacement/ L | 12.939 |
| Compression ratio | 11 : 1 |
| Rated power/ kW | 338 |
| Rated speed/ r/min | 1900 |

a) One-dimensional Numerical Simulation of Miller Cycle

Generally speaking, in order to optimize the intake and exhaust process, the intake valves are

usually closed after bottom dead center (ABDC), EIVC or LIVC of Miller cycle discussed here is based on the intake valve close timing of original cycle which is 22°CA ABDC, not the top dead center. Six kinds of Miller cycle are proposed on the first ground, including three EIVC and three LIVC, the valve lifting curves are shown in Figure 2.

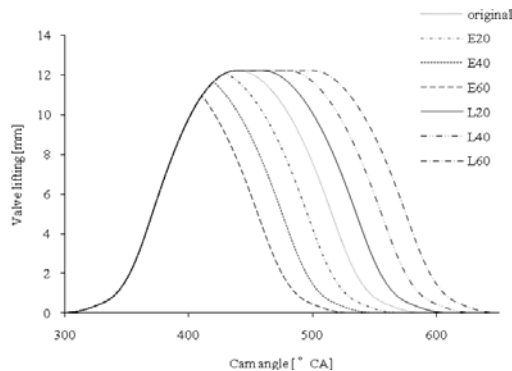


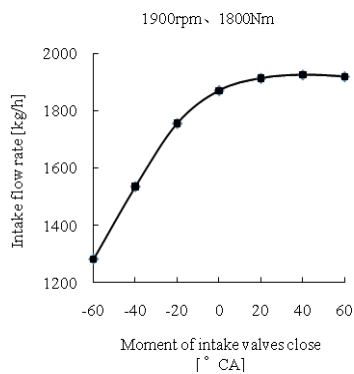
Figure 2: Six Kinds of Miller Cycle

EIVC20, intake valve close timing is at 2°CA ABDC; EIVC40, intake valve close timing is at 18°CA ABDC; EIVC60, intake valve close timing is at 38°CA ABDC; LIVC20, intake valve close timing is at 42°CA ABDC; LIVC40, intake valve close timing is at 62°CA ABDC; LIVC60, intake valve close timing is at 82°CA ABDC.

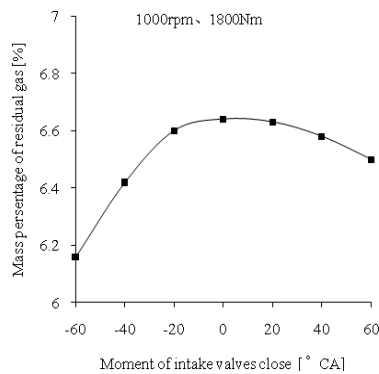
The one-dimensional model was built with the software of GT-POWER, and the heat release rate model was Weber function, the heat transfer model was Woschni 1978.

i. Calculation Results

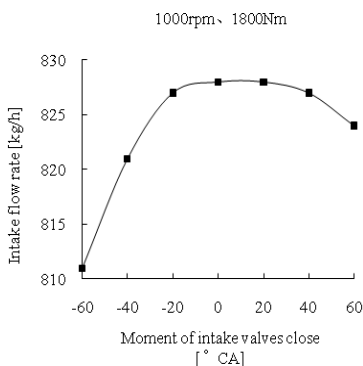
Changes of the amount of intake charge are shown in figure 3, "-60" on the abscissa indicates E60, "60" indicate L60. Keeping the opening of turbocharger bypass constant, miller cycles change the amount of intake charge. For 1900r/min, due to the longer time for intake, the later the valves close, the more charge the engine gets. Compared to the original cycle, the intake of E20, E40 and E60 decrease by 6.1%, 18% and 31.5% respectively, but intake charge doesn't change a lot from L20 to L60. For 1000r/min, EIVC's influence is not as much as 1900r/min. So in the six Miller cycles, EIVC has more influence than LIVC on the intake amount, and EIVC has more influences at the high speed working condition than the low speed working condition.



(a)



(b)

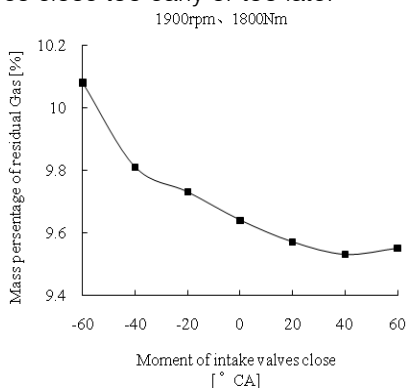


(b)

Figure 3: Change of Intake Mass Flow

ii. Change of Residual Gas

Figure 4 shows the change of residual gas of miller cycles. For high speed condition, the later the intake valves close, the less the amount of the residual gas, due to the longer time for scavenging. For low speed condition, the residual gas decreases when the intake valves close too early or too late.



(a)

Figure 4: Change of Residual Gas

Generally speaking, the cam profile of the exhaust valve has a greater effect to the residual gas than the intake valve, Figure 5 shows the change of the residual gas according to the exhaust phase, it can be seen that, when the exhaust phase is postponed 10 ~ 20°CA, the mass fraction of residual gas reaches the smallest value. Theoretically, minimizing the residual gas is an effective measure to broaden the knock limit.

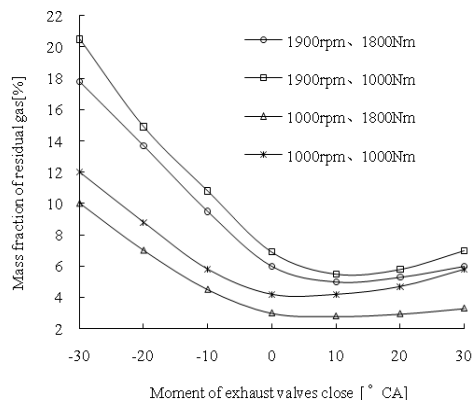
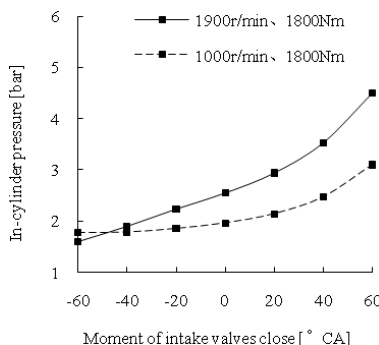


Figure 5: Change of Residual Gas with Different Exhaust Valve Close Timing

iii. Change of in-cylinder pressure and temperature when the intake valves close

The in-cylinder pressure and temperature at the time of intake valves closing both increase while the intake valves close later, as Figure 6 shows.



(a)

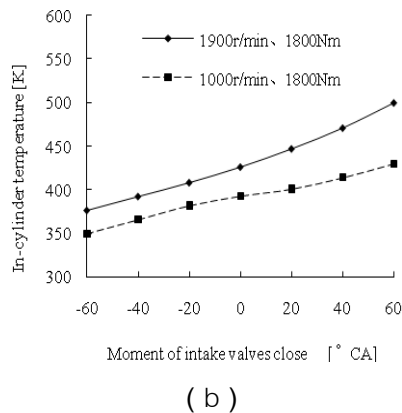


Figure 6: change of in-cylinder pressure and temperature when the intake valves close

iv. Change of Intake Temperature

In the case of LIVC, some of the intake charge is pushed reversely into the induct, and the compression work converted into internal energy of the fresh charge in the intake ports, which makes the intake temperature of next cycle increases, as shown in Figure 7. On the contrary, intake temperature drops obviously for EIVC because of the expansion before compression. The purpose of this paper is to reduce the compression temperature by Miller cycle, Figure 7 shows that LVIC doesn't hit the mark, so in the subsequent analysis only EVIC is taken into account.

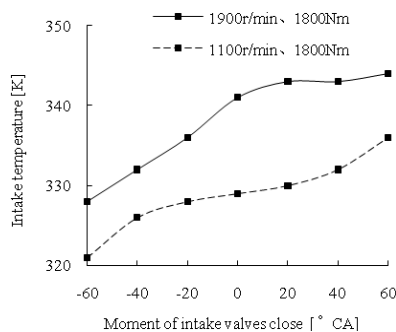


Figure 7: Changes of Intake Temperature

Through the above one-dimensional simulations, we can see that EVIC changes the intake process and decreases the in-cylinder pressure and temperature when the intake valves close, which help to reduce the maximum combustion temperature and detonation tendency, so higher compression ratio is possibly to be employed to improve the thermal efficiency. On the other hand, EVIC changes the state of air-fuel mixture, that will also changes the combustion efficiency, especially when the temperature of the mixture drops, the combustion speed will decrease, and the thermal efficiency will decrease also, so it is necessary to do further analysis for in-cylinder processes by multidimensional numerical simulation.

b) Multidimensional numerical simulation of in-cycle cylinder flow and combustion of EVIC

Large eddy simulation (LES) and G equation flamelet model are employed to investigate the in-cycle cylinder flow and combustion of different EVICs.

i. Large Eddy Simulations

When LES is used, the flow variables are decomposed into two parts, the large-scale motions that are supported by the mesh size and the small, sub-grid scale (SGS) motions that are less than the grid size. Spatial filtering is applied to both the variables and the governing equations, leading to governing equations for the resolved large-scale motions. The governing equations can be written as the following^[3,4]:

$$\begin{aligned} \frac{\partial \bar{p}}{\partial t} + \frac{\partial \bar{\rho} \bar{u}_i}{\partial x_i} &= 0 \\ \frac{\partial \bar{\rho} \bar{u}_i}{\partial x_i} + \frac{\partial \bar{\rho} \bar{u}_i \bar{u}_j}{\partial x_j} &= -\frac{\partial \bar{p}}{\partial x_i} + \frac{\partial \bar{\tau}_{ij}}{\partial x_j} + \frac{\partial}{\partial x_j} (\bar{\rho} \bar{u}_i \bar{u}_j - \overline{\rho u_i u_j}) \\ \frac{\partial \bar{\rho} \bar{h}}{\partial t} + \frac{\partial \bar{\rho} \bar{h} \bar{u}_j}{\partial x_j} &= \frac{\partial \bar{p}}{\partial t} + \frac{\partial}{\partial x_j} \left(\bar{\rho} D \frac{\partial \bar{h}}{\partial x_j} \right) + \frac{\partial}{\partial x_j} (\bar{\rho} \bar{h} \bar{u}_j - \overline{\rho h u_j}) \end{aligned} \quad (1)$$

Where ρ is the density of the mixture; u_i is the velocity component in the x_i direction (1, 2, 3); p is the pressure; τ_{ij} is the viscous stress tensor; D is the thermal diffusion coefficient; and h is the enthalpy. The overbars denote spatially-filtered quantities, whereas over-tildes denote the density-weighted spatially-filtered quantities. For example,

$$\begin{aligned} \bar{p}(x_i, t; \Delta) &= \int_{-\infty}^{\infty} \int_{-\infty}^{\infty} \int_{-\infty}^{\infty} F(x_i - x'_i; \Delta) \rho(x'_i, t) \\ \tilde{h}(x_i, t; \Delta) &= \frac{1}{\bar{\rho}} \int_{-\infty}^{\infty} \int_{-\infty}^{\infty} \int_{-\infty}^{\infty} F(x_i - x'_i; \Delta) \rho(x'_i, t) h(x'_i, t) d^3 \zeta \end{aligned} \quad (2)$$

Where F is a filter function and Δ is the filter width (here taken as the cell size). The last term in Eq.(2) is the SGS stress whereas the last term in Eq.(3) is the turbulent transport flux that accounts for the effect of the un-resolved sub-grid turbulence. The SGS stresses are modeled here using the scale-similarity model^[5,6], whereas the SGS scalar transport fluxes are modeled by Smagorinski model.

An equation of state is used to couple the pressure, temperature and density in the cylinder. The calorific equation of state is used to compute the temperature of the fluid from the enthalpy. In the present engine test, the in-cylinder flow speed is less than 120 m/s and the Mach number is lower than 0.3. For simplicity, in Eq. (3) the 'low Mach number approximation' has been used. With this approximation, the pressure is split into two parts, a hydrodynamic pressure and a thermodynamic pressure. The former is responsible for the pressure gradient that drives the flow, in Eq. (2). The latter depends on time (or the crank

angle) only. It is used in the equation of state to couple with the density and temperature.

ii. Ignition Model

To spark ignition engines, the current numerical grid scale is too large to capture the small structure of the initial phase of the fire kernel, so fire kernel growth in this paper is described by the discrete particle ignition kernel model(DPIK)^[7].

$$\frac{dr_k}{dt} = \frac{\rho_u}{\rho_k} (S_T + S_{plasma}) + \frac{1}{3} r_k \left(\frac{1}{T_k} \frac{dT_k}{dt} \right) \tag{3}$$

where r_k is the radius of the fire kernel; ρ_u is the density of the burned fire kernel; S_{plasma} is the Plasma growth rate; T_k is the temperature inside the fire kernel S_{plasma} is calculated by:

$$S_{plasma} = \frac{Q_{electr}}{4\pi r_k^2 \left[\rho_u (U_k - H_u) + p \frac{\rho_u}{\rho_k} \right]} \tag{4}$$

Where Q_{electr} is ignition energy; U_k is the internal energy of the kernel; H_u is the enthalpy of the unburned charge; P is the in-cylinder pressure.

When the kernel is larger than several times the Integral length scale L_I , i.e. $r_{k2} \geq C_k L_I$ (usually $C_k = 2.5$), the combustion calculation switches to G equation flamelet model.

iii. G-equation Flamelet Turbulent Flame Propagation Model

G-equation combustion model based on flamelet theory of premixed combustion, in which turbulent flames are considered a series of laminar flames, and a G-field whose level $G = G_0$ represents the flame surface, is introduced to simulate the propagation affront of premixed turbulent flame. The G - equation and the Navier-Stokes equations integrate into the description of turbulent premixed combustion flame front propagation, which can be written after being filtered[8]:

$$\frac{\partial \bar{G}}{\partial t} + \mathbf{u} \cdot \nabla \bar{G} = S_T^0 |\nabla \bar{G}| - \overline{D\kappa} |\nabla \bar{G}| \tag{5}$$

where \mathbf{u} is the flow velocity; S_L^0 is the turbulent flame speed, which has to be modeled; D is the diffusivity; κ is the flame stretch ratio.

Turbulent flame speed is modeled by:

$$\frac{S_T^0 - S_L^0}{u'} = - \frac{a_4 b_3^2}{2b_1} Dal^* + \sqrt{\left(\frac{a_4 b_3^2}{2b_1} Dal^* \right)^2 + a_4 b_3^2 Dal^*} \tag{6}$$

Where $a_4 = 0.78$, $b_1 = 2.0$, $b_3 = 0.1$, S_L^0 is the laminar flame speed, Da is the Damköhler number, l^* is the process variable which indicates the relationship between the degree of development of turbulent flame and time, it can be written:

$$l^* = \left[1 - \exp\left(-2.0 \frac{t}{t_i}\right) \right]^{\frac{1}{2}} \tag{7}$$

Where t is the initial moment and tt is the time being considered.

The Simulation is performed on the software of KIVA. An engine mesh of medium grid density was built with the same geometry as the real engine, as figure 8 shows. The calculation point is 1900r/min-1800Nm, the excess air ratio is 1.5, a spark plug located at the center of the combustion chamber, ignition timing is 20°CA before top dead center.

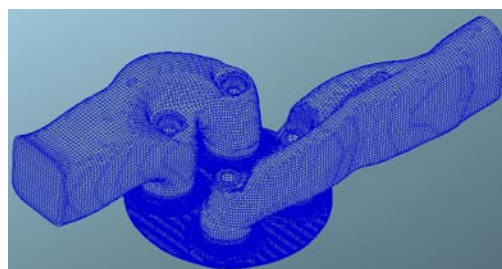
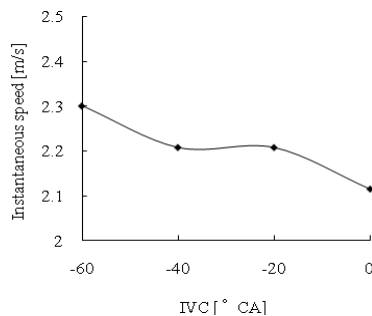


Figure 8: The gid of Model

c) Calculation Results

Figure 9 shows the change of turbulence parameters at the time of ignition around the spark plug. When the intake valve closed early, the instantaneous speed increases, which is in favor of the initial flame propagation; the integral length scale increases slightly, it means that EIVC makes the flame be more inclined to propagate at a laminar speed at the first moment; on the other hand, the fluctuation velocity and the turbulent kinetic energy decrease, Which go against the rapid spread of flame.



(a)

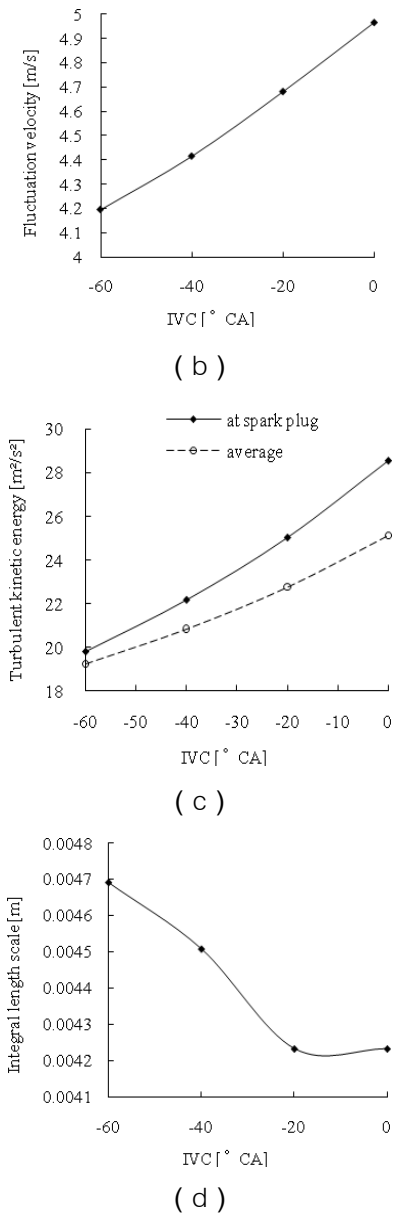


Figure 9: Comparison of Turbulence Parameters at Spark Ignition at 1900r/min, 1800Nm

Figure 10 shows the heat release, in-cylinder pressure and temperature during combustion. With the intake valves closing early, the heat release lags behind and becomes slow, so the burst pressure and the maximum temperature decrease. E20 doesn't make much difference and the in-cylinder pressure decreases too much for E60.

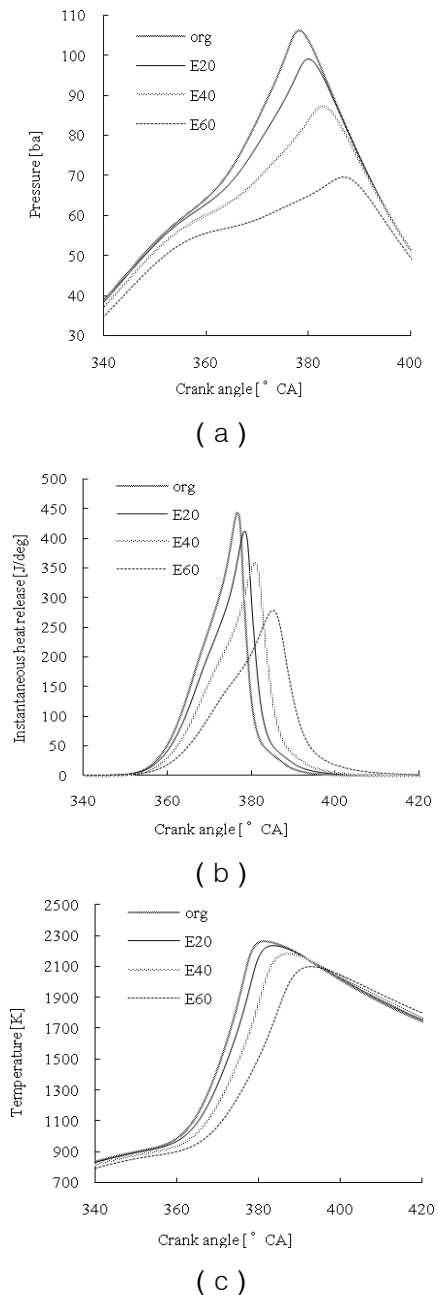


Figure 10: Burning and Heat Release at 1000r/min, 1800Nm

According to the above simulation, E40 has a lower combustion temperature and a relatively rapid combustion process compared with the original cycle, so it is chosen as a scheme to improve the gas engine's performance. Miller cycle decreases the combustion temperature, so the geometry compression ratio can be improved to optimize the engine's performances. And the next step is to optimize the compression ratio.

d) Optimization of compression ratio

The original compression ratio is 11, and the chamber profile is shown in Figure 11. Modify the main

structural parameters D and H to increase the geometric compression ratio to 12 and 13, as shown in table 2. Table 3 compares the calculated main turbulence parameters with different compression ratios at the ignition time under the condition of 1900r/min-1800N, it shows that the locate turbulence parameters don't change a lot when the compress ratio changes.

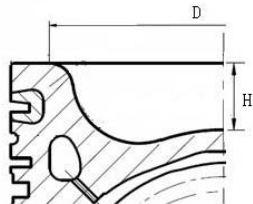


Figure 11: Sketch of Piston

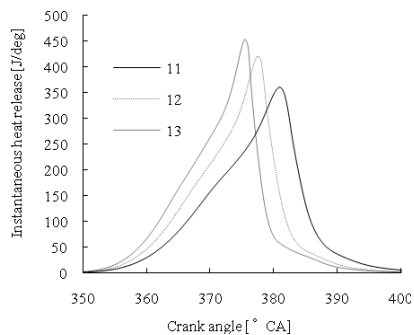
Table 2: Main Parameters of Piston with Different Compression Ratio

| 压缩比 | D (m) | H (m) |
|-----|---------|---------|
| 11 | 0.118 | 0.024 |
| 12 | 0.114 | 0.023 |
| 13 | 0.109 | 0.022 |

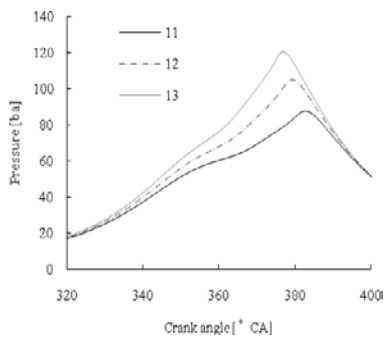
Table 3: The Main Turbulence Parameters around the Plug at 20°C BTDC

| Compression ratio | 11 | 12 | 13 |
|------------------------------------|---------|---------|---------|
| Turbulence Kinetic energy (m2/s) | 34.7 | 34.7 | 36.3 |
| Flow velocity (m/s) | 2.42 | 2.54 | 2.65 |
| Integral length scale (m) | 0.00496 | 0.00492 | 0.00488 |

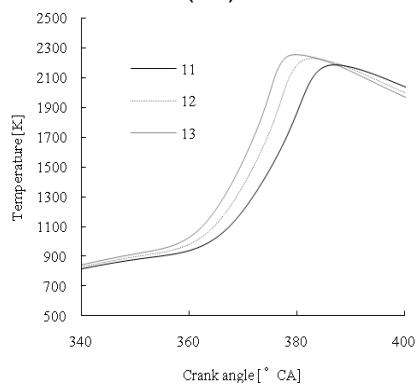
Figure 12 shows the in-cylinder parameters under different compression ratios at 1900r/min-1800Nm. The higher the compression ratio, the faster the combustion heat release, the higher the boost pressure, and the maximum temperature in the cylinder. Compared to 11, the maximum instantaneous heat release rate, the highest pressure and the maximum temperature raise by 3.2%, 38.1% and 25.9% respectively when the compress ratio raises to 13. In this paper, we focus on the potential of improving the thermal efficiency, so the compression ratio 13 is chosen to used in E40 in the following experiment.



(b)



(a)



(c)

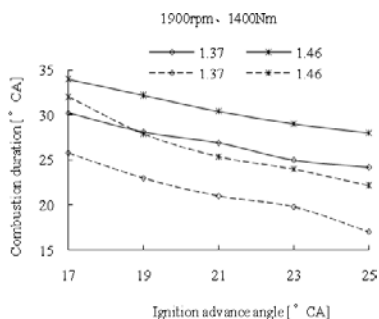
Figure 12: Pressure, Heat Release and temperature at 1900r/min, 1800Nm

IV. EXPERIMENTAL RESULTS

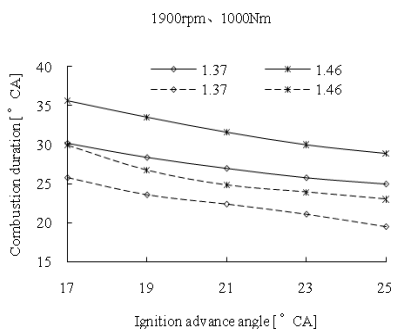
In the test research, in order to optimize the performance, the boost pressure, excess air coefficient, ignition advance angle are carefully chosen for each working condition, the comparisons of the experimental results between original cycle and miller cycle are given below.

a) *Combustion Duration*

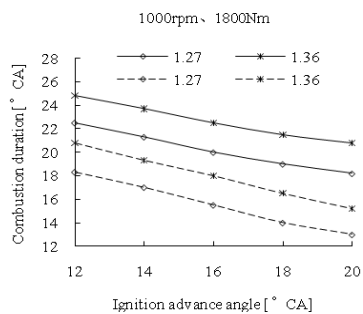
Figure 13 shows the comparison of the combustion duration (10%~90%) which varies according to the excess air coefficient and the ignition advance angle. It can be seen that the Miller cycle has a shorter combustion period. At 1900r/min, the combustion duration of the Miller cycle is about 5°C shorter; at 1000rpm, the combustion duration of the Miller cycle is about 4°C shorter.



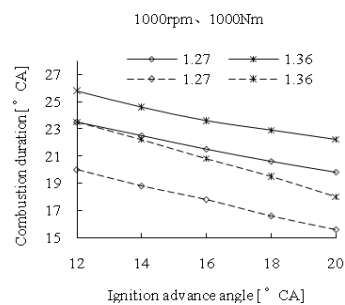
(a)



(b)



(c)

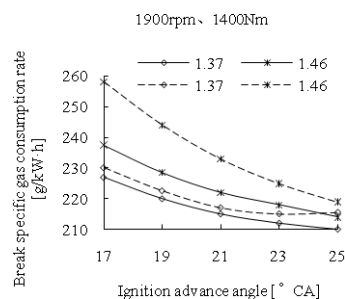


(d)

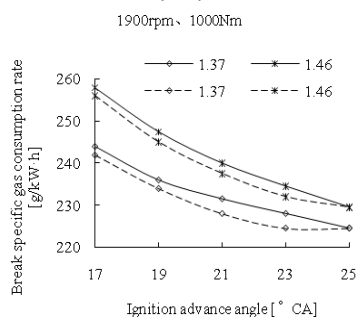
Figure 13: Comparison of the Burning Duration

b) *The Performance of Miller Cycle*

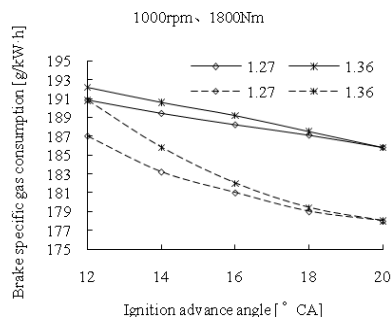
Figure 14 shows the comparison of the break specific gas consumption, at 1900r/min, when the load is above 1400Nm, due to the lower volume efficiency and more residual gas, the miller cycle has a higher gas consumption; under 1400Nm, miller cycle has a less gas consumption because of the reduction of cycle charge, At 1000r/min, the specific gas consumption of miller cycle obviously decreases, about 7~8g/kw.h.



(a)



(b)



(c)

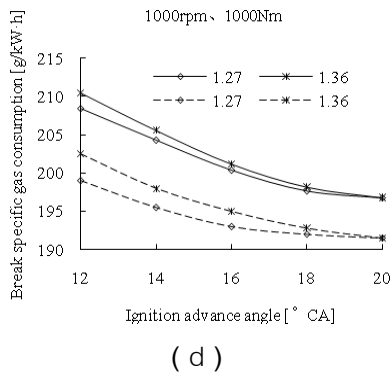


Figure 14: Comparison of Break Specific Gas Consumption

Figure 15 shows the comparison of the thermal efficiency. At high speed condition, thermal efficiency doesn't have much difference, but at low speed condition, The thermal efficiency of the Miller cycle is about 5~7% higher, the maximum thermal efficiency of the Miller cycle reached 47%, the increase of thermal efficiency is mainly caused by the higher compression ratio, while the residual gas coefficient has great influence on the thermal efficiency of the high speed.

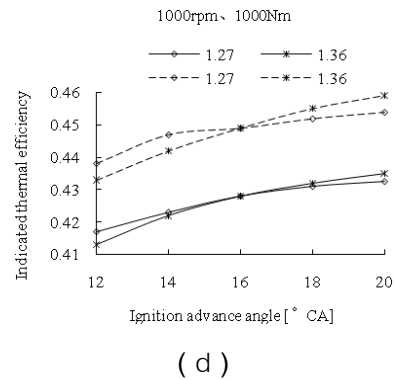


Figure 15: Comparison of Thermal Efficiency

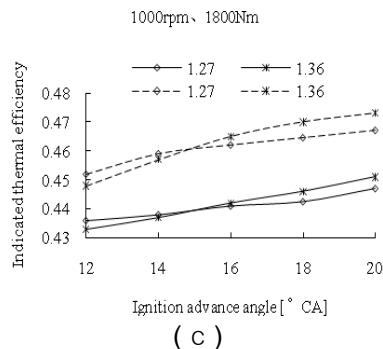
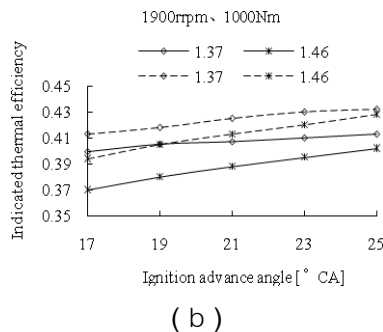
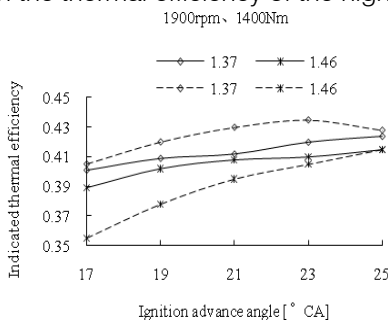
V. CONCLUSION

The simulation calculation of the Miller system which combines EIVC with higher compression ratio is carried out, and the heat release process is investigated in detail, according to the calculation results, the optimization scheme is selected and put into experimental study. Compared to the original cycle, the optimization scheme has the following characteristics:

- 1) the pumping loss is slightly lower.
- 2) the heat release is relatively concentrated and rapid, the combustion center is about 5 °CA earlier, and the time for the combustion duration decreases by 5 °CA, so the thermal efficiency increases.
- 3) The break specific gas consumption of the middle and low speed improves obviously, but in the condition of high speed and heavy load, it is deteriorated due to the increase of the residual exhaust gas.

REFERENCES RÉFÉRENCES REFERENCIAS

1. M. Furno Palumbo. (2007). CFD-Analysis of intake-system performances of a small turbocharged spark-ignition engine. *SAE paper 2007-24-0047*.
2. Puzinauskas P V, Willson B D and Evans K H. (2000). Optimization of natural gas combustion in sparkignited engines through manipulation of intake-flow configuration. *SAE paper 2000-01-1948*.
3. Kato T, Saeki K, Nishide H and Yamada T. (2001). Development of CNG fueled engine with lean burn for small size commercial van. *JSAE Rev 1, 1, 365-368*.
4. Reza Rezaei, Stefan Pischinger, Jens Ewald and Philipp Adomeit. (2010). A New CFD Approach for Assessment of Swirl Flow Pattern in HSDI Diesel Engines. *SAE paper 2010-32-0037*.
5. Stefano Fontanesi, Giuseppe Cicalese and Elena Severi. (2013). Analysis of Turbulence Model Effect on the Characterization of the In-Cylinder Flow Field in a HSDI Diesel Engine. *SAE paper 2013-01-1107*.



6. Das A and Watson HC. (1997). Development of a natural gas spark ignition engine for optimum performance. *Proc Inst Mech Eng, Part D: J Automobile Engineering* 2, 3, 361–378.
7. Li F and Reitz R D. (2000). Development of an ignition and combustion model for spark-ignition engines. *SAE Paper* 2000-01-2809.
8. H. Pitsch. (2002). A G-equation formulation for large-eddy simulation of premixed turbulent combustion. Center for Turbulence, *Research Annual Research Briefs* 5, 4, 3-14.

GLOBAL JOURNALS INC. (US) GUIDELINES HANDBOOK 2016

WWW.GLOBALJOURNALS.ORG